processes

MDPI

Article

Modified Mixed-Integer Linear Programming Formulation Implemented in Microsoft Excel to Synthesize a Heat Exchanger Network with Multiple Utilities to Compare Process Flowsheets

Maria F. Revelo [1] and Pablo V. Tuza [2,*]

[1] Unidad Educativa Rafael León Carvajal, Ministerio de Educación, Distrito Educativo Intercultural y Bilingüe 10D03 Cotacachi, Coordinación Zonal 1, Cotacachi 100306, Ecuador; maferevelocb@gmail.com
[2] Facultad de Ciencia e Ingeniería en Alimentos y Biotecnología, Universidad Técnica de Ambato, Ambato 180216, Ecuador
* Correspondence: pv.tuza@uta.edu.ec; Tel.: +593-2400987

Abstract: In the present work, a modified mixed-integer linear programming model was implemented in Microsoft Excel® and minimized using the Solver tool to obtain information to devise a heat exchanger network with multiple utilities from a set of hot and cold streams and selected utilities by hand. Regarding the mixed-integer linear programming problem, the summation of utility energy was added to the model, and this energy was equal to that from the Temperature Interval method and the Grand Composite Curve. Moreover, feasible temperature ranges for heat exchange were considered according to the second law of thermodynamics. Also, the last two temperature intervals from the rank-ordered ones were assigned for water energy balances. An energy balance was introduced into the algorithm for each interval between its temperature and the process pinch temperature in the case of the boiler-feed water. Seven stream sets collected from the literature were used for the mixed-integer linear programming formulation testing, and six of them are presented in this article. Because of boiler-feed water generation and the low cost of utilities, the annualized cost of a heat exchanger network with multiple utilities can be lower than that of a network without multiple utilities.

Keywords: pinch; heat exchanger network; multiple utilities; mixed-integer linear programming; Microsoft Excel

Citation: Revelo, M.F.; Tuza, P.V. Modified Mixed-Integer Linear Programming Formulation Implemented in Microsoft Excel to Synthesize a Heat Exchanger Network with Multiple Utilities to Compare Process Flowsheets. *Processes* **2023**, *11*, 2840. https://doi.org/10.3390/pr11102840

Academic Editor: Marek Markowski

Received: 15 August 2023
Revised: 20 September 2023
Accepted: 25 September 2023
Published: 27 September 2023

1. Introduction

Commodities like ammonia or hydrogen can be obtained by utilizing the Stage-Gate Technology Development Process (SGTDP) methodology before the Stage-Gate Product Development Process (SGPDP) procedure [1]. The latter method comprises concept, feasibility, manufacture, development, and product introduction. Concerning SGTDP, it is formed by technology scoping, technology assessment, and technology transfer. Therefore, eight levels must be passed before the product is launched into the market.

Process synthesis for the chemical species mentioned above occurs at the concept level, which is made up of five steps: (i) chemical reaction; (ii) mixing, recycling, and division streams; (iii) separation steps; (iv) pressure and temperature changes; and (v) equipment substitution. Finally, heat integration, including high, medium, and low-pressure steam and boiler-feed water (BFW) incorporation, is applied to the fourth step [1].

Fuel (F), steam (S), and water (W) are some required utilities in the industry for heating and cooling process streams in a heat exchanger network (HEN). It should be mentioned here that the heat from hot i streams that cannot raise the temperature of process streams or generate BFW is dumped into the W utility. In contrast, the heat can be stored by performing a gas–gas, liquid–gas, or solid-gas chemical reaction, concentrating and then diluting chemical species, or harnessing ammoniated salt pairs, hydrated salt pairs, or metal hydrides, as described by Yan et al. [2]. Similarly, rocks, ceramics, and molten salts can be utilized for this goal [3]. All of these options are influenced by temperature, and they enable the saving of waste energy.

A HEN is obtained by minimizing a mixed-integer nonlinear programming (MINLP) formulation from different superstructure (SST) assessments. In this case, Yee and Grossman [4] addressed a stage-wise SST considering possible heat exchanges between the i and cold j streams. Furthermore, Nair and Karimi [5] reviewed an SST with a pool of two-stream heat exchangers (HEs). Likewise, Sun et al. [6] communicated a stage-wise SST accounting for the generation and absorption processes from a compression–absorption cascade refrigeration system. Also, Rathjens and Fieg [7] used a genetic algorithm and deterministic local optimization techniques for solving the SST. In addition, the HEN obtention by solving a MINLP using results from the resolution of mixed-integer linear programming (MILP) problems of the same process-stream data has been claimed by Nemet et al. [8], with optimization of the temperatures, flowrates, and areas associated with each match by Caballero et al. [9]. The GAMS program has been handled for model optimization [4–6,8,9].

On the other hand, there are several measures of profitability to compare process flowsheets at the Task Integration level [1], and they can depend on the area of HEs and the utilities. These two parameters can be obtained by determining the minimum amount of utilities using the Temperature Interval (TI) method and then the minimum number of HEs following a MILP approach. The sequential mode comprises these last two strategies [10], and the area can be obtained from heat loads associated with the minimum number of HEs. It is worth mentioning that (i) the exact values of the capital and operating costs at the Task Integration level are not necessary [11], and (ii) the sequential mode provides a value near the corresponding optimum [12]. Therefore, the sequential mode is adequate to compare process flowsheets.

In the process design stage, the inclusion of multiple utilities in the HEN can be manually carried out after the HEN synthesis [13], evaluating the Grand Composite Curve [14] as published for a chemical process [15]. Conversely, other strategies for multiple utilities introduced into the HEN have been communicated in the literature. For example, Yeo et al. [16] proposed a graphical method to determine the minimum utility values and the minimum number of HEs in which phase changes occur. Additionally, Ponce-Ortega et al. [17] developed a MINLP strategy from an SST, including different types of utilities. Moreover, Na et al. [18] communicated a utility substage in a stage-wise SST.

Some computer programs have been employed to solve problems involving the incorporation of multiple utilities into HENs. For instance, Papoulias and Grossmann [19] reported the synthesis of HENs with multiple utilities in assessing a MILP framework in the LINDO software. In this last work, the pinch process and the pinch utilities are determined simultaneously. Furthermore, Shenoy et al. [20] synthesized HENs with multiple utilities as a function of the Total Annual Cost by setting up the HXTARG software.

Microsoft Excel® has been widely applied in the determination of Minimum Energy Recovery (MER) values from a set of i and j streams [21], obeying the Problem Table Algorithm spreadsheet [22], or the Goal Seek function [23], and HEN design [24]. In this situation, Walmsley et al. [25] found a novel HEN retrofit targeting method for the HEN design in configuring this software.

To the best of our knowledge, the multiple utilities determined by the TI method or the Grand Composite Curve, the minimum heat transferred between i and j streams according to the second law of thermodynamics, the assignment of two last intervals for the W utility to collect the heat, and energy balances per interval between the process pinch and the BFW pinch have not been taken into account in the MILP model. As a solution, the Microsoft Excel® program was used to obtain a HEN with the minimum amount of HEs, the MER requirements, their cost, and the annualized cost (C_A). This methodology could be utilized to select a process flowsheet at the Task Integration level. In this context, this work aims to report the synthesis of HENs with multiple utilities and their C_A, yearly utility costs (C_U), and purchase costs (HEN C_P) by assessing a modified version of the conventional MILP approach and the Microsoft Excel® program to compare process flowsheets.

2. Problem Statement

In the design stage, for a given set of i and j streams with their source and target temperatures, their product of flow rate and heat capacity, i.e., the C value, the utility streams, their cost, the ΔT_{min} value, and the HE C_P, a HEN with selected multiple utilities, the minimum number of HEs, the MER targets, and the lowest value of C_A are obtained. Figure 1 illustrates a flowchart indicating the obtention of HEN for all examples solved in this work, showing its connection with the modified MILP (m-MILP) framework and input data.

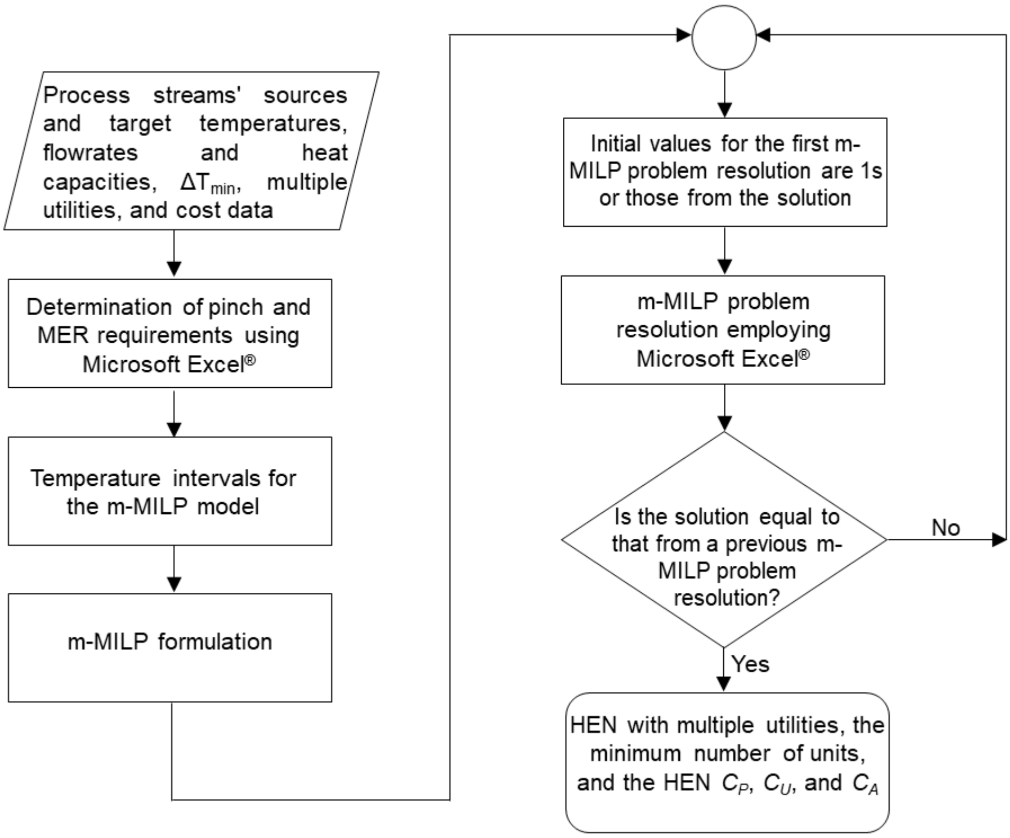

Figure 1. Flowchart depicting the HEN synthesis with multiple utilities, the C_U, HEN C_P, and C_A, and their relation to the m-MILP algorithm and process-streams information, multiple utilities, and cost data.

3. Methodology

3.1. Problem Formulation

The TI method [1] was carried out to determine the pinch temperature and the MER objectives. In addition, the Large function was used to rank the temperatures for temperature interval obtention. Concerning the C value per interval (Equation (1)) operation (C_H and C_C are C values for i and j streams, respectively), Equation (2) was employed. Without considering their bounds, if a common temperature between the interval formed by the adjusted source and target temperatures of a process stream and a temperature interval determined by the TI method is detected, its C value is considered for Equation (1). It is worth pointing out that a constant value of heat capacity and no phase change in any process streams or utilities were assumed [26].

$$(\text{CI}) = \sum C_H - \sum C_C \tag{1}$$

formula = IF(Y(condition1; condition2); value_if is true; value_if is false) (2)

The rank-ordered intervals required for the m-MILP approach were derived from the source temperature of process streams [1]. These temperatures were placed in the vertices of a stack with same-size squares: the source temperatures of i streams were set at the left side stack, while the source temperatures of j streams were at the right side stack. Since the intervals are represented by horizontal lines in the stack, which depict the ΔT_{min} value, the other temperatures for each interval were obtained by aggregating (source temperatures of j streams) or subtracting (source temperatures of i streams) the ΔT_{min} value. For example, the temperature intervals obtained for a hypothetical set of two i and two j streams are presented in Figure S1 of the Supplementary Material. In this last figure, the pinch temperature was indicated by a horizontal line to show the limit for heat flow that comes from intervals at higher temperatures. Likewise, the i and j streams were qualitatively located at the left and right side square stacks, respectively.

The W utility source temperature was assumed to be 15 °C [27]. Similarly, its target temperature was equal to the second-lowest source temperature of j streams minus 1. This previous procedure defines the W-utility C value and guarantees a heat remotion by the W utility in the last two intervals. After obtaining the MER targets, the pinch temperature, and the temperature intervals for the m-MILP problem, the transshipment model [19] was used to create a modified formulation compared to that of the minimum HEs obtention [1], coupled with forbidden matches between i and j streams or without process pinch, as proposed by Biegler et al. [10]. The m-MILP algorithm is the following:

$$\begin{gathered} \min z = \sum_i \sum_j y_{ij} \\ w.r.t. \\ Q_{ijk},\ y_{ij} \\ s.t. \end{gathered} \tag{3}$$

$$\begin{gathered} R_{ik} + \sum_{j \in C_k} Q_{ijk} - R_{i,k-1} - Q^H_{ik} = 0\ i \in H_k, \\ k = 1, \ldots, K \end{gathered} \tag{4}$$

$$\sum_{i \in H_k} Q_{ijk} - Q^C_{jk} = 0\ j \in CS_k,\ k = 1, \ldots, K \tag{5}$$

$$\sum_k Q_{ijk} - y_{ij} U_{ij} \le 0\ i \in H,\ j \in CS \tag{6}$$

$$\sum_k Q^H_{UUk} = UU^H \tag{7}$$

$$R_{ik} \ge 0,\ Q_{ijk} \ge 0,\ y_{ij} \in 0,1 \tag{8}$$

An important remark is that, through their residuals, the i streams can transfer heat to the j streams at intervals where they are absent [1]. Regarding the inclusion of BFW utility, an energy balance was implemented for each interval formed between the process pinch temperature and its utility temperature.

It is important to note that the utility U_{ij} (Equation (6)) means the lowest heat exchanged between the i and j streams. This definition is opposite to the one elaborated by Seider et al. [1], who determined U_{ij} values that are not according to the second law of thermodynamics. In the case of the match i-BFW, contrasting the heat of i streams per interval and BFW heat from the Grand Composite Curve, the U_{ij} values were determined. Equation (7) guarantees that the utility heat introduced at all k intervals equals the value determined by the TI method or the Grand Composite Curve [1]. In this case, one equation per hot utility must be introduced into the m-MILP algorithm.

3.2. m-MILP Problem Solution

All the computer calculations were performed using Microsoft Excel® 2016. Also, the GRG Nonlinear method from the Solver tool was selected to solve the m-MILP algorithm, applying the default parameter settings of the program. It is essential to point out that if there are problems with convergence on a solution, the Evolutionary method can be employed instead of the GRG Nonlinear method [28]. Furthermore, the starting values were 1 for the first m-MILP model solving. In addition, the Solver execution was carried out until the solution values were equal to those from a previous resolution of the same m-MILP formulation. The time for the last m-MILP resolution is communicated for each example carried out in this investigation. Lastly, the m-MILP approach solution provides information to devise the HEN manually with and without multiple utilities.

3.3. HEN C_P, C_U, and C_A

Cost data for determining the HEN C_P, C_U, and C_A are shown in Table 1. Since BFW production reduces energy consumption to produce the S utility [29], this can be considered an income. Thus, the BFW cost was subtracted from the C_U.

As developed by Seider et al. [1], the flowsheets' C_A values for the same heating and cooling task can be compared, and as a result, its formula (Equation (9), Table 1) was exploited in this work. Similarly, a value of 1 for F_P, F_M, and F_L (Equation (10), Table 1), and F_T and an overall heat-transfer coefficient of 444 W m^{-2}K^{-1} [30] (Equation (13), Table 1) were found suitable to obtain a mathematical expression that depends only on the area, as proposed in work by Liu et al. [31]. Moreover, because of its low price, the Fixed-Head HE was used (Equation (11), Table 1) [32]. Related to the C_P, since its mathematical relationship (Equation (11), Table 1) is valid for the range of 13.9 to 1114.8 m^2, this range's lowest limit was assumed for areas less than this value. On the other hand, if the area was above the range, it was divided into equal parts equivalent to 1114.8 m^2 or less [33]. Furthermore, the C_P was updated with the index cost corresponding to December 2022 [34] (Equation (10), Table 1). Additionally, Equation (12) enables the logarithmic mean temperature calculation, even for those cases where the temperature difference value from i stream inlet minus j stream outlet (ΔT1) equals that from i stream outlet minus j stream inlet (ΔT2). It is worth noting that the HEN C_P is computed by summing each HE C_P and configuring the HEN.

Table 1. Cost data and formulae for obtaining the HEN C_P, C_U, and C_A.

Parameter	Value or Formula	No. of Equation	Reference
Water, 15 °C	USD 10 (kW y)$^{-1}$		[27]
BFW, 110 °C	USD 14.14 (kW y)$^{-1}$		[1]
Steam, 170 °C	USD 57.14 (kW y)$^{-1,\ a}$		[35]
Steam, 226.85 °C	USD 106.85 (kW y)$^{-1,\ a}$		[10]
High-pressure steam, 280 °C	USD 160 (kW y)$^{-1}$		[27]
Steam, 332.25 °C	USD 164.63 (kW y)$^{-1,\ a}$		[1]
Fuel, 800 °C	USD 200 (kW y)$^{-1}$		[27]
Annualized cost	$C_A = i_m(C_{TCI}) + C_U$	(9)	[1]
HE f.o.b. purchase cost	$C_P = F_P F_M F_L C_B \left(\frac{I}{I_{base}}\right)$	(10)	[1]
Fixed head HE base f.o.b. purchase cost	$C_B = exp\left\{11.0545 - 0.9228[ln(A)] + 0.09861[ln(A)]^2\right\}$	(11)	[36]
Chen's approximation of the logarithmic mean temperature	$\Delta T_{LM} = [\Delta T1\, \Delta T2\, 0.5\, (\Delta T1 + \Delta T2)]^{1/3}$	(12)	[37]
Heat exchanged in a HE	$Q = UAF_T\Delta T_{LM}$	(13)	[38]

[a] This cost was obtained by cost data interpolation from Chang et al. [27].

4. Examples

4.1. Example 1

Table S1 depicts a set of two hot and two cold streams reported by Seider et al. [1] and the multiple utilities introduced to the HEN. Moreover, Tables S2 and S3 present the above streams' pinch determination and MER requirements at the minimum temperature difference (ΔT_{min}) value of 10 °C. Furthermore, the m-MILP model comprised 24 energy balances, 31 continuous variables, 14 binary variables, 33 constant parameters, and 14 restrictions describing possible HEs involving utilities and process streams (Tables S11–S15). It is important to note that the constant parameters include the heat of i streams provided to j streams for each interval and the minimum amount of heat exchanged between themselves within their temperature range, obeying the second law of thermodynamics, i.e., Q_{ik}^{H}, Q_{jk}^{C}, and U_{ij}, respectively. In addition, the time resolution for the m-MILP problem was about 10 s. Figure 2 illustrates the HEN with multiple utilities, which shows 12 HEs, with a C_A of USD 26,025.16 (Row 2, Table 2). An essential remark is that detailed information for this example is indicated in SM Figure S6.

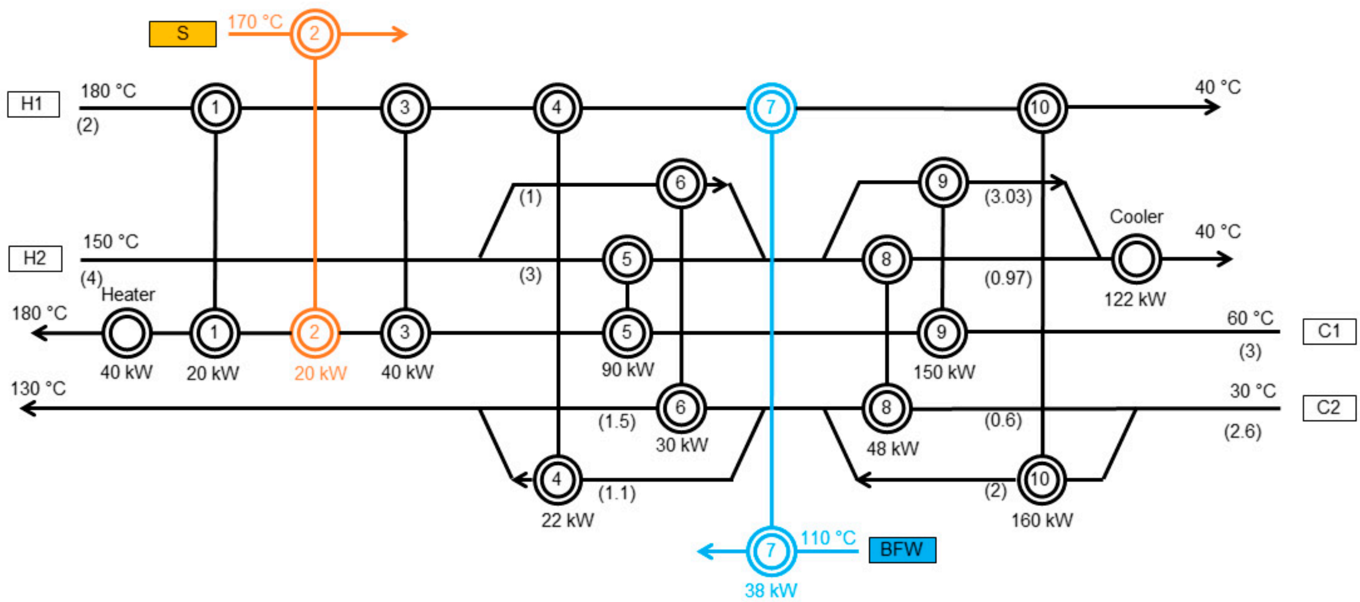

Figure 2. HEN with multiple utilities for Example 1. ΔT_{min}: 10 °C. S pinch temperature: 170 °C. Process pinch temperature: 140 °C. BFW pinch temperature: 110 °C. C_A: USD 26,025.16. C values are also in parenthesis and possess kW °C^{-1} units.

Table 2. BFW cost, C_U, HEN C_P, and C_A for Examples 1 to 6.

Example	BFW	C_U		HEN C_P		C_A	
	(USD)	(USD)	(%) [a,b]	(USD)	(%) [a]	(USD)	(%) [a]
1 [c]		7600	30.5	97,108.57	51.9	17,310.86	33.5
1 [d]	537.38	5825.47		201,996.88		26,025.16	
2 [c]		43,510.6	18.3	124,810.2	46.2	55,991.62	6.6
2 [d]		36,784.2		231,790.37		59,963.24	
3 [c]		11,343,897.21	13.8	423,221.79	20.8	11,386,219.39	13.6 [b]
3 [d]	302,552.77	9,971,022.68		534,268.95		10,024,449.58	
4 [c]		53,889.55	17.4	98,368.64	26.9	63,726.41	7.4 [b]
4 [d]		45,897.6		134,550.92		59,352.69	

Table 2. *Cont.*

Example	BFW	C_U		HEN C_P		C_A	
	(USD)	(USD)	(%) [a,b]	(USD)	(%) [a]	(USD)	(%) [a]
5 [c]		2,191,360	30.7	183,511.99	19.1	2,209,711.2	30 [b]
5 [d]		1,676,745.84		226,735.23		1,699,419.36	
6 [c]		191,500	16.7	192,909.67	42.3	210,790.97	6.7 [b]
6 [d]	14,141.7	164,158		334,436.19		197,601.92	

[a]: 100 (Value from HEN with multiple utilities cost—Value from HEN without multiple utilities cost)/Value from HEN with multiple utilities cost (14). [b]: Absolute value. [c]: Value from HEN without multiple utilities. [d]: Value from HEN with multiple utilities.

The HEN without multiple utilities is exhibited in SM Figure S3. It contains six HEs, as proposed by Seider et al. [1]. This last result is an insight into the methodology accuracy reported in this article. Although the HEN C_P and C_A were increased by 51.9% and 33.5%, respectively, the C_U was reduced by 30.5% in the case of the HEN with multiple utilities compared to the same HEN without multiple utilities (see Row 2 from Table 2).

4.2. Example 2

Table S18 shows the set of streams for Example 2 to obtain a HEN with multiple utilities at the threshold approach temperature difference ($\Delta T_{threshold}$). Similarly, the pinch temperature and the MER requirements are indicated in Tables S19 and S20. It is essential to note that this example has no pinch temperature for integer values below 50 °C; thus, this last temperature is the $\Delta T_{threshold}$ [39]. Likewise, the m-MILP formulation comprised 38 energy balances, 71 continuous variables, 25 binary variables, 51 constant parameters (accounting for Q^H_{ik}, Q^C_{jk}, and U_{ij}), and 25 inequalities for possible HEs (Tables S28–S32). For this example, the computation time was about 180 s. A critical remark is that this was achieved after several attempts to get initial guesses for obtaining the same m-MILP problem resolution. This solution is composed of 13 HEs and is depicted in Figure 3. Additionally, the C_A was equal to USD 59,963.24 (Row 4, Table 2). It should be mentioned that Figure S11 presents temperatures between the HEs and more significant figures for C values and heat loads for this example.

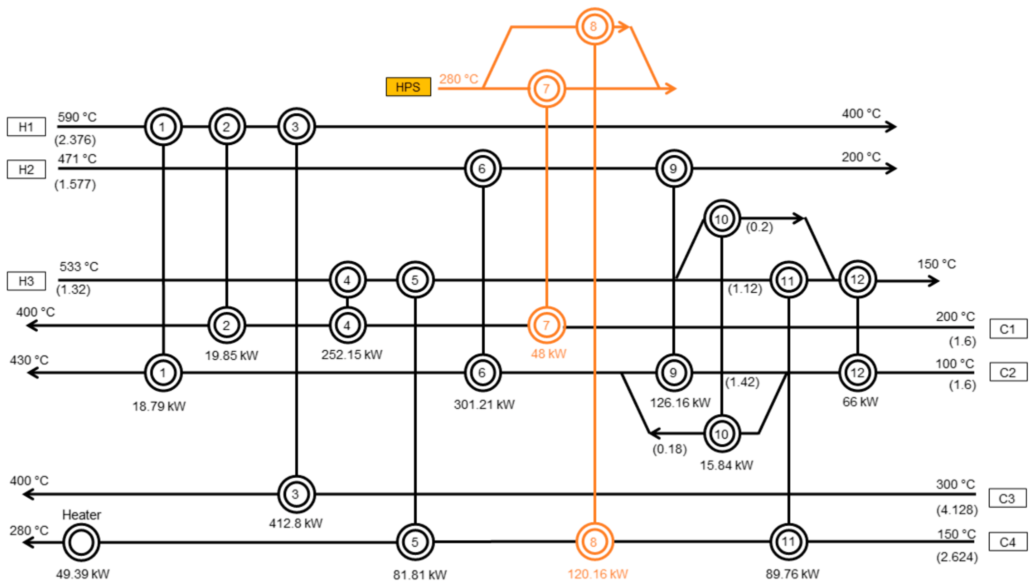

Figure 3. HEN with multiple utilities for Example 2. $\Delta T_{min} = \Delta T_{threshold}$: 50 °C. HPS pinch temperature: 280 °C. Process pinch temperature: 100 °C. C_A: USD 59,963.24. Furthermore, the C values are in parenthesis with kW $°C^{-1}$ units.

Seider et al. [1] communicated the HEN for this example using only the S utility and the Stream Matching Rules at the pinch. These authors claimed seven HEs for the HEN. On the contrary, in the findings of this research, the HEN without multiple utilities is illustrated in SM Figure S8. Although the total number of HEs was equal to those reported by Seider et al. [1], the number of utility HEs was lower. As represented in Table 2, even though C_A and HEN C_P increased by 6.6% and 46.2%, the C_U was reduced by 18.3%.

4.3. Example 3

Regarding the third example, the ten streams Mizutani et al. [34] employed were used to obtain the HEN with multiple utilities. The C values, source, target temperatures, and selected utilities are also illustrated in Table S35. Likewise, the pinch determination and the MER objectives with a ΔT_{min} value of 10 K are presented in Tables S36 and S37. After solving the m-MILP model for the HEN without multiple utilities, 15 HEs were found (Table S43). However, these HEs did not comprise a HEN adhering to the C rule at the pinch and ΔT_{min} values greater or equal to 10 K for HEs involving C2 at the hot side of the process pinch. Although the minimum HEs C_P will not be achieved as indicated in the tick-off heuristic [40], to accommodate the heat needed by C2 to reach its target temperature, the heat loads for each interval were incorporated progressively for the cases of intervals 4, 5, and 6.

On the left side of the process pinch, C2 was divided five times to place the heat from S, H3, H4, H5, H6, and H7 in C2 (Rows 3 and 12–16, Table S44). Similarly, in the case of the heat provided by S to C2 at interval 6, as represented in Figure S13a, it was added after HE 10 since the obtained outlet temperature is close to 473 K when compared to those achieved after placing this load at outlets 9, 11, 12, or 13 HEs. It is worth noting that isothermal temperature is recommended at the mixing stage, as shown in work by Seider et al. [41], to minimize the magnitude of the irreversibilities and, thus, the value of the generated entropy [42]. Therefore, the C2 temperature was increased from 423 K to 473 K. Then, the heat loads from S, H4, H5, H6, and H7 were transferred to C2 at Interval 5 (Rows 2 and 8–11, Table S44) to obtain a C2 temperature of 523 K. Next, the heat from H5 and H7 was introduced to C2 (Rows 5–6, Table S44) at Interval 4. Finally, the new total number of HEs for the HEN without multiple utilities was 22.

Regarding the HEN with multiple utilities, the values of the m-MILP problem resolution are depicted in Tables S46–S50. It comprises 56 energy balances, 123 variables, 73 constant parameters (related to Q^H_{ik}, Q^C_{jk}, and U_{ij}), and 34 restrictions illustrating feasible HEs between i and j streams. Also, the resolution time was about 240 s. In addition, the number of HEs was 23. Since this was insufficient to be in accordance with the C rule and the ΔT_{min} restriction of 10 K on the hot side of the process pinch, the heat transfer between i and j streams for each interval was performed for those matches involving C2 on the side of the process pinch mentioned above, as carried out for this example without multiple utilities. HEs 4 and 7 to 16, obtained through this last procedure, are represented by the green color in Figure 4a. Since BFW receives heat from H2 at intervals 8 and 9, only one HE was employed. The total number of HEs was 28, as depicted in Figure 4, with detailed findings in Figure S16 and a C_A of USD 10,024,449.58 (Row 6, Table 2).

As shown in Table 2, the HEN C_P increased by 20.8%. However, a reduction of C_A (13.6%) and C_U (13.8%) was observed, which can be attributed to the high BFW production, costing USD 302,552.77 per year, and the low cost of the S utility.

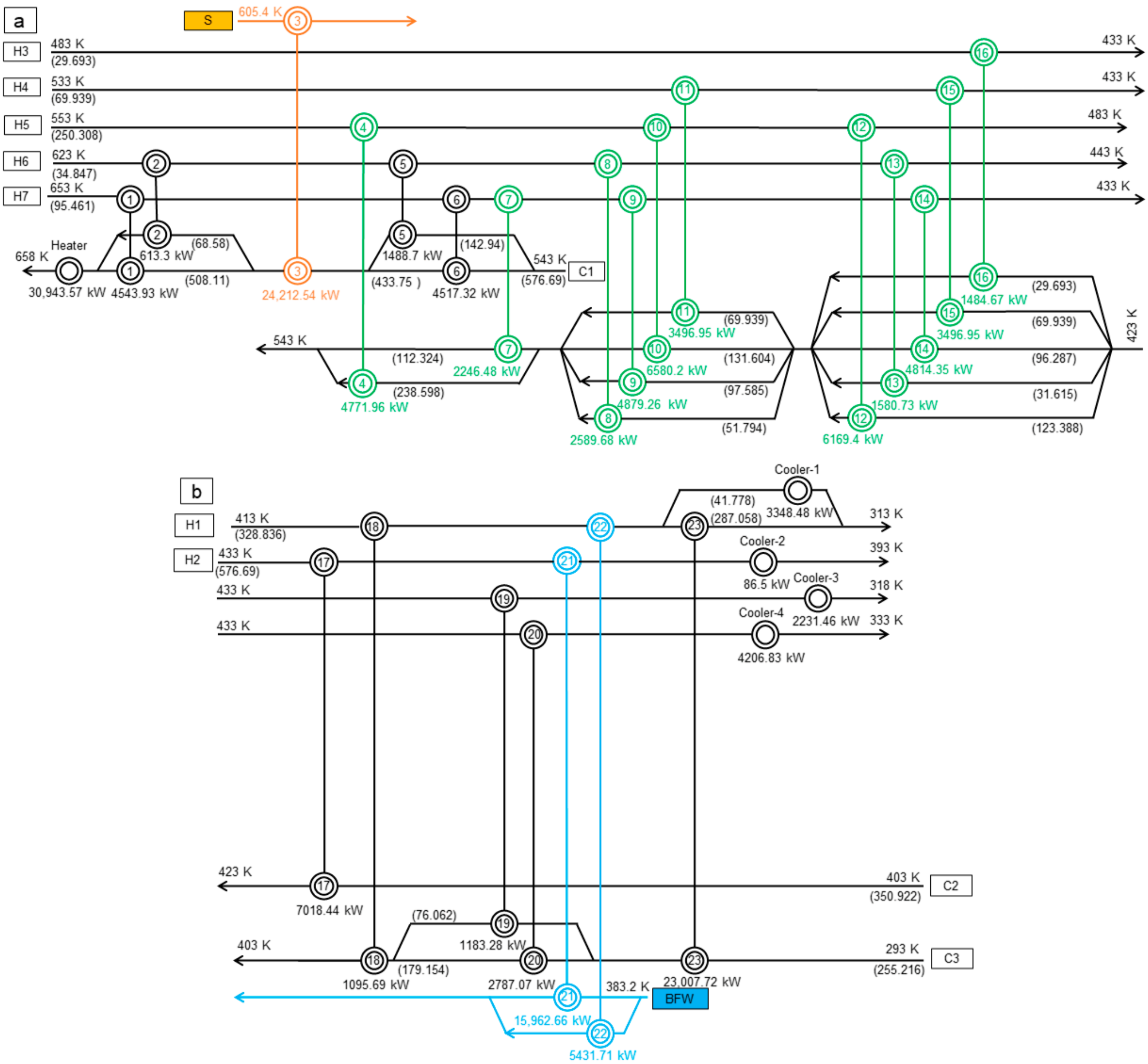

Figure 4. HEN with multiple utilities for Example 3: (**a**) hot and (**b**) cold sides from the process pinch. ΔT_{min}: 10 K. S pinch temperature: 605.4 K. Process pinch temperature: 423 K. BFW pinch temperature: 383.15 K. C_A: USD 10,024,449.58. Moreover, the C values are indicated in parenthesis and present kW K^{-1} units.

4.4. Example 4

For this example, a HEN with multiple utilities displaying two process pinch temperatures devised at the $\Delta T_{threshold}$ is obtained using the methodology tested in this work. The HEN without multiple utilities and designed at the $\Delta T_{threshold}$ was proposed by Seider et al. [1]. The process streams and utilities are indicated in Table S54, and they consist of five i streams and one j stream, including HPS and S at 500 K. Also, the MER requirements and the process pinch temperatures are depicted in Table S56. In this table, it can be observed that, at the $\Delta T_{threshold}$ of 25.833 K, the heat provided by the HPS utility was 336.81 kW, and the process pinch temperatures were 468.47 K and 451.67 K, the same as reported by Seider et al. [1].

The m-MILP comprised 15 energy balances, 29 variables, 21 constant parameters, and nine restrictions describing possible HEs. The time resolution of this model was about 10 s.

Furthermore, the results involved nine HEs with a C_A of USD 59,352.69, as exhibited in Figure 5 and Figure S21, with more values for this last illustration.

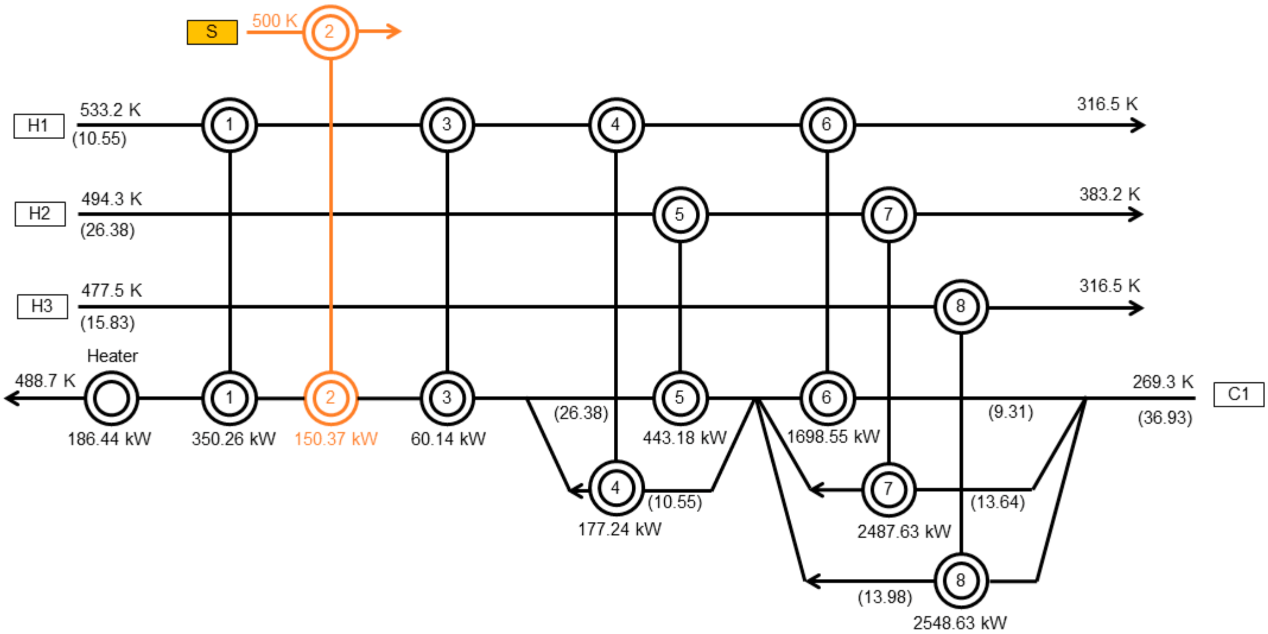

Figure 5. HEN with multiple utilities for Example 4. $\Delta T_{min} = \Delta T_{threshold}$: 25.833 K. S pinch temperature: 500 K. First-process pinch temperature: 468.47 K. Second-process pinch temperature: 451.67 K. C_A: USD 59352.69. Furthermore, the C values are in parenthesis with kW K^{-1} units.

The HEN without multiple utilities is presented in SM Figure S18, and it comprises seven HEs, as found in the literature [1]. Finally, the HEN C_P, C_U, and C_A are represented in Table 2. Contrasting to the HEN without multiple utilities, the HEN with multiple utilities showed C_U and C_A reductions of 17.4% and 7.4%, respectively, due to the low cost of the S utility.

4.5. Example 5

This example illustrates the combination of the m-MILP results and the Solver tool from Microsoft Excel® to derive information to draw a HEN with multiple utilities by hand. In addition, the data set containing the source and target temperatures and C values for five i and one j streams (Table S71) was initially published by Jiang et al. [43]. Furthermore, the utilities F and S at 332.25 °C were employed for this example. Likewise, at the ΔT_{min} of 10 °C, the F heat was 10,956.8 kW, and the process pinch temperature was 52 °C (Table S73).

For the case of the HEN without multiple utilities, the m-MILP encompassed 28 energy balances, 51 variables, 25 constant parameters, and six restrictions for possible matches between i and j streams (Tables S74–S78). The time computation for this algorithm resolution was about 10 s. Although the results from the m-MILP depicted six HEs (Table S79), more than these units were used for the HEN without multiple utilities. This number increased because, after placing the F heat in the C1 stream to achieve the C1 target temperature and then splitting this cold stream into five streams, the summation of each branch-C value from those five streams was not equal to the C1-C value of 143.9 kW $°C^{-1}$. Therefore, the heat of i streams in the sixth interval from Figure S22 was introduced to C1, enlarging the HEs number compared to that achieved by solving the m-MILP algorithm (Table S79).

The procedure for heat addition in the sixth interval to the C1 stream was as follows: (i) After the placement of the F heat from intervals 1 to 5 of Figure S22 to C1 and dividing it into five branches, the heat of the i streams in the sixth interval was exchanged to the C1 stream. It is worth pointing out that an inlet heater temperature of 284.4 °C (Figure S23) was accomplished with this previous step. The sixth interval contains the process pinch temperature of 52 °C and the temperature difference of 144 °C (Figure S22) for cold streams.

(ii) Except for the branch case with the lowest heat load, the branch-C value was calculated by dividing the heat load by the temperature difference of 144 °C. (iii) The remaining branch-C value was obtained by subtracting each branch-C value obtained in the previous step from 143.9 kW $°C^{-1}$. (iv) In this final branch, the heat from the F utility in the sixth interval was incorporated at the outlet of the match i–j to obtain a temperature of 196 °C, which is respective from the other branches' outlet in the sixth interval.

Next, as described in Figure S23, the heat from the fifth interval was transferred to C1, assuming the above procedure for the sixth interval, attaining a C1 temperature of 220 °C. Regarding the heat from intervals lower or equal to the fourth interval, it was possible to utilize this energy and the temperatures of 220 °C and 284.4 °C to obtain branch-C values whose summation was equal to that of the C1 by handling the Solver tool. This last mathematical operation was the objective function. In this case, the ΔT1 value greater or equal to 10 °C was a restriction for the branch-C values' computation, which were 86.36 kW $°C^{-1}$, 23.46 kW $°C^{-1}$, and 34.08 kW $°C^{-1}$. Finally, the number of HEs was 12.

For the HEN with multiple utilities, the equations, variables, constant parameters, and restrictions representing the m-MILP model are exhibited in Tables S82–S86. It employed about 10 s for the m-MILP resolution. The procedure to identify matches between i streams and C1 for devising the HEN without multiple utilities by hand was followed to obtain the HEN with multiple utilities. This last HEN presented 16 HEs, a C_A value of USD 1,699,419.36, and is shown in Figure 6, with details in Figure S26.

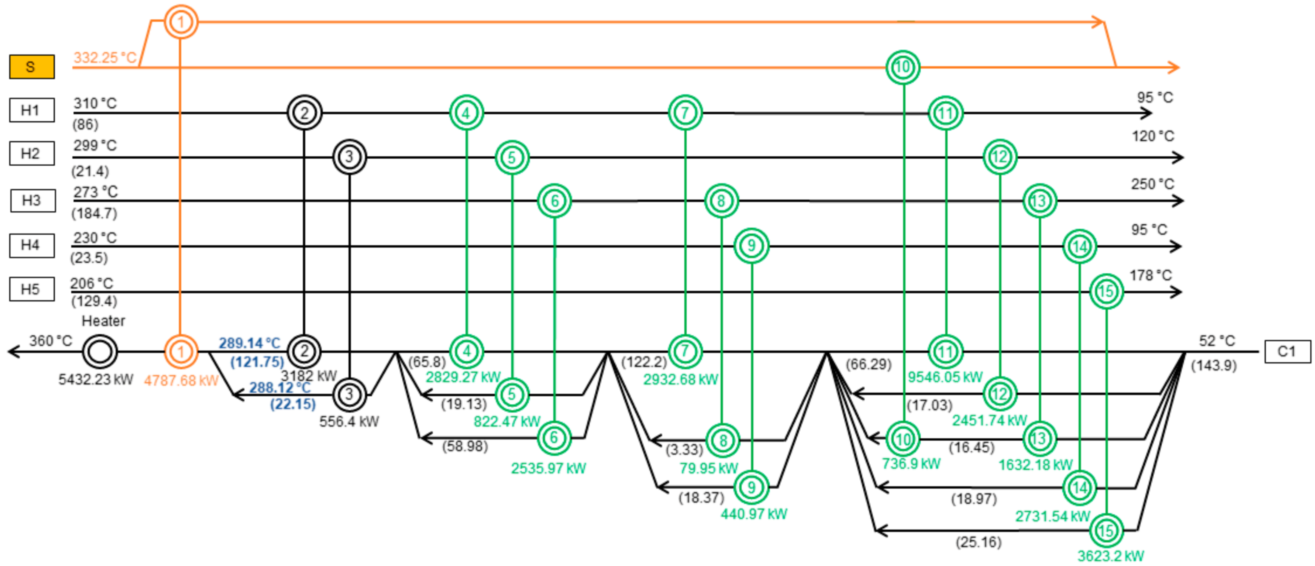

Figure 6. HEN with multiple utilities for Example 5. ΔT_{min} = 10 °C. S pinch temperature: 332.25 °C. Process pinch temperature: 52 °C. C_A: USD 1,699,419.36. Furthermore, the C values are in parenthesis with kW $°C^{-1}$ units.

In Figure 6, the green 4 to 15 HEs illustrate the transfer of i streams of heat per interval to C1. Moreover, the blue numbers next to HEs 2 and 3 in Figure 6 indicate the C values and temperatures obtained using the Solver tool from Microsoft Excel®. Finally, the HEN C_P, C_U, and C_A are displayed in Table 2. Though the HEN C_P increased, the C_U and C_A were reduced by 30.7% and 30%, respectively, ascribed to the low cost of the S utility.

4.6. Example 6

This example describes the m-MILP model application for two intervals between the process and BFW pinches involved in the problem. Similarly, the set of streams is exhibited in Table S90 and includes four i streams and one j stream. This information was reported by Seader et al. [1]. Likewise, the F and HPS utilities were utilized for this example.

Also, at the ΔT_{min} value of 10 °C, the F heat was 900 kW, whereas the process pinch was 250 °C, and the heat received by W was 1150 kW (Table S92). The m-MILP model for this example with multiple utilities is presented in Tables S101–S105. It includes 41 energy balances, 107 continuous and discrete variables, 65 constant parameters, and 35 restrictions representing possible matches between i and j streams. Moreover, the time resolution for this problem was about 60 s, and the results are shown in Figure 7, with a C_A of USD 197,601.92. Another essential remark is that there are more decimal places for the values in Figure S31 than in this last figure, and temperatures between the HEs make up Figure S31.

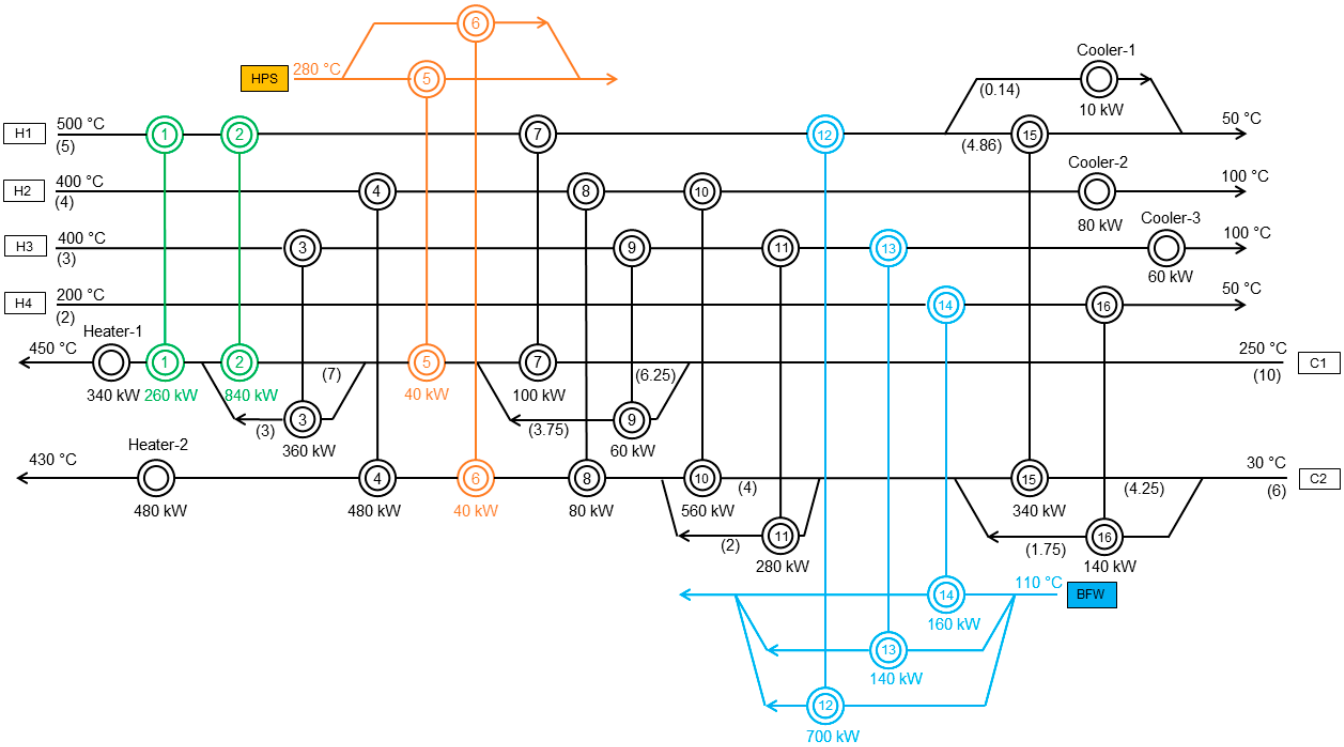

Figure 7. HEN with multiple utilities for Example 6. ΔT_{min} = 10 °C. HPS pinch temperature: 280 °C. Process pinch temperature: 250 °C. C_A: USD 197,601.92. Furthermore, the C values are in parenthesis with kW °C^{-1} units.

Since a ΔT1 value of at least 10 °C for the match H1-C1 above the HPS pinch (Rows 4 and 5, Table S106) was impossible to obtain, the green HEs 1 and 2 from Figure 7 were employed to illustrate this last match. In addition, the blue HE 12 from Figure 7 indicates the two consecutive matches between H1 and BFW (Rows 17 and 18, Table S106). On the other hand, concerning the model solution for this example without multiple utilities, the Tables S93–S97 comprise the m-MILP model. It used the Evolutionary method for the first set of results from the m-MILP model resolution. Subsequently, this method was switched to the GRG Nonlinear method to solve the problem.

Table 2 depicts the effect of the addition of multiple utilities in the HEN C_P, C_U, and C_A from the HEN without multiple utilities. Even though the HEN C_P was increased by 42.3%, the C_U and C_A costs were reduced by 16.7% and 6.7%, respectively. This decrease is attributed to BFW production and the low cost of the HPS utility.

5. Conclusions

In this work, a modified mixed-integer linear programming problem was implemented in Microsoft Excel® to synthesize heat exchanger networks with multiple utilities. In this model, energy balances account for the heat loads provided or received by utilities, which were equal to the corresponding duty from the Temperature Interval method and the Grand Composite Curve. Also, the last two intervals from those rank-ordered were assigned for water to collect the heat from hot streams. Furthermore, the minimum amount of heat transferred between a hot and a cold stream adheres to the second law of thermodynamics. Regarding the boiler-feed water generation, an energy balance per temperature interval was employed between the process pinch and the boiler-feed water pinch. In addition, the annualized cost for a heat exchanger network with multiple utilities can be lower than its counterpart without multiple utilities because of boiler-feed water production and the low cost of utilities.

Supplementary Materials: The following supporting information can be downloaded at: https://www.mdpi.com/article/10.3390/pr11102840/s1, Figure S1: Temperature intervals derivation for the m-MILP problem. Example 1: Figures S2–S6; Tables S1–S17. Example 2: Figures S7–S11; Tables S18–S34. Example 3: Figures S12–S16; Tables S35–S53. Example 4: Figures S17–S21; Tables S54–S70. Example 5: Figures S22–S26; Tables S71–S89. Example 6: Figures S27–S31; Tables S90–S108.

Author Contributions: Conceptualization, M.F.R. and P.V.T.; methodology, M.F.R. and P.V.T.; software, M.F.R. and P.V.T.; validation, M.F.R. and P.V.T.; formal analysis, M.F.R. and P.V.T.; investigation, M.F.R. and P.V.T.; resources, M.F.R. and P.V.T.; data curation, M.F.R. and P.V.T.; writing—original draft preparation, P.V.T.; writing—review and editing, M.F.R. and P.V.T.; visualization, M.F.R. and P.V.T.; supervision, P.V.T.; project administration, P.V.T.; funding acquisition, P.V.T. All authors have read and agreed to the published version of the manuscript.

Funding: This research received no external funding.

Data Availability Statement: Not applicable.

Acknowledgments: Pablo V. Tuza acknowledges Universidad Técnica de Ambato/Ecuador for supporting this work.

Conflicts of Interest: The authors declare no conflict of interest.

Nomenclature

Abbreviations	
BFW	Boiler-feed water
F	Fuel
HE	Heat exchanger
HEs	Heat exchangers
HEN	Heat exchanger network
HENs	Heat exchanger networks
HPS	High-pressure steam
MER	Minimum energy recovery
MILP	Mixed-integer linear programming
MINLP	Mixed-integer nonlinear programming
m-MILP	Modified mixed-integer linear programming
MPS	Medium-pressure steam
S	Steam
SGPDP	Stage-gate product development process
SGTDP	Stage-gate technology-development process
SM	Supplementary material
SST	Superstructure
TI	Temperature Interval method
W	Water
Symbols	
A	The area for the heat transfer
C	Product of flow rate and heat capacity
C_A	Annualized cost
C_B	Fixed head heat exchanger base f.o.b. purchase cost
C_C	C values for cold streams
C_H	C values for hot streams

CS	The set of cold streams (or set of cold utilities)
CI	C value per interval from the Temperature Interval method
C_P	Heat exchanger f.o.b. purchase cost
C_U	Annual utility cost
C_{TCI}	Total capital investment
F_L	Length factor
F_M	Material factor
F_P	Pressure factor
F_T	Correction factor
H	The set of hot streams (or set of hot utilities)
i	Hot process stream (or hot utility)
I	Updated index cost
I_{base}	Base index cost
i_m	Annual return on investment
j	Cold process stream (or cold utility)
k	Interval index
K	Last interval determined by the process pinch (or utility pinch)
Q	Heat exchanged in a unit
Q_{ik}^H	Heat provided by a hot stream (or hot utility) at k interval
Q_{ijk}	Heat exchanged by a hot stream (or hot utility) and a cold stream (or cold utility) at k interval
Q_{jk}^C	Heat received by a cold stream (or cold utility) at k interval
Q_{UUk}^H	Hot utility per interval
R_{ik}	Hot stream (or hot utility) residual at k interval
ΔT_{LM}	Chen's approximation of the logarithmic mean temperature
ΔT_{min}	Minimum temperature difference
$\Delta T_{threshold}$	Threshold approach temperature difference
$\Delta T1$	Inlet temperature of hot stream (or hot utility) minus outlet temperature of cold stream (or cold utility)
$\Delta T2$	Outlet temperature of hot stream (or hot utility) minus inlet temperature of cold stream (or cold utility)
U	Overall heat-transfer coefficient
U_{ij}T	Minimum amount of heat exchanged between a hot stream (or hot utility) and a cold stream (or cold utility), limited by the process pinch or utility pinch, and according to the second law of thermodynamics
UU^H	Hot utility value determined by the Temperature Interval method or the Grand Composite Curve
y_{ij}	1 for a feasible match between a hot stream (or hot utility) and a cold stream (or cold utility), or 0 when there is no match between a hot stream (or hot utility) and a cold stream(or cold utility)
z	Objective function value

References

1. Seider, W.D.; Seader, J.D.; Lewin, D.R.; Widagdo, S. *Product and Process Design Principles*, 3rd ed.; John Wiley and Sons: Hoboken, NJ, USA, 2009; pp. 3–604.
2. Yan, T.; Wang, R.Z.; Li, T.X.; Wang, L.W.; Fred, I.T. A review of promising candidate reactions for chemical heat storage. *Renew. Sustain. Energy Rev.* **2015**, *43*, 13–31. [CrossRef]
3. Gunasekara, S.N.; Barreneche, C.; Inés Fernández, A.; Calderón, A.; Ravotti, R.; Ristić, A.; Weinberger, P.; Ömur Paksoy, H.; Koçak, B.; Rathgeber, C.; et al. Thermal energy storage materials (TESMs)—What does it take to make them fly? *Crystals* **2021**, *11*, 1276. [CrossRef]
4. Yee, T.F.; Grossmann, I.E. Simultaneous optimization models for heat integration—II. Heat exchanger network synthesis. *Comput. Chem. Eng.* **1990**, *14*, 1165–1184. [CrossRef]
5. Nair, S.K.; Karimi, I.A. Unified Heat Exchanger Network Synthesis via a Stageless Superstructure. *Ind. Eng. Chem. Res.* **2019**, *58*, 5984–6001. [CrossRef]
6. Sun, X.; Liu, L.; Zhuang, Y.; Zhang, L.; Du, J. Heat exchanger network synthesis integrated with compression–absorption cascade refrigeration system. *Processes* **2020**, *8*, 210. [CrossRef]
7. Rathjens, M.; Fieg, G. Cost-optimal heat exchanger network synthesis based on a flexible cost functions framework. *Energies* **2019**, *12*, 784. [CrossRef]

8. Nemet, A.; Isafiade, A.J.; Klemeš, J.J.; Kravanja, Z. Two-step MILP/MINLP approach for the synthesis of large-scale HENs. *Chem. Eng. Sci.* **2019**, *197*, 432–448. [CrossRef]
9. Caballero, J.A.; Pavão, L.V.; Costa, C.B.B.; Ravagnani, M.A.S.S. A Novel Sequential Approach for the Design of Heat Exchanger Networks. *Front. Chem. Eng.* **2021**, *3*, 40. [CrossRef]
10. Biegler, L.T.; Grossmann, I.E.; Westerberg, A.W. *Systematic Methods of Chemical Process Design*; Prentice Hall: Upper Saddle River, NJ, USA, 1999; pp. 533–546.
11. Serth, R.W. *Process Heat Transfer: Principles and Applications*; Academic Press: Burlington, VT, USA, 2007; p. 329.
12. Turton, R.; Bailie, R.C.; Whiting, W.B.; Shaeiwitz, J.A.; Bhattacharyya, D. *Analysis, Synthesis and Design of Chemical Processes*, 4th ed; Prentice Hall: Upper Saddle River, NJ, USA, 2012; p. 500.
13. Towler, G.; Sinnott, R. *Chemical Engineering Design Principles, Practice and Economics of Plant and Process Design*, 2nd ed.; Elsevier: Oxford, UK, 2013; p. 147.
14. Shenoy, U.V. *Heat Exchanger Network Synthesis: Process Optimization by Energy and Resource Analysis*; Gulf Publishing Company: Houston, TX, USA, 1995; p. 61.
15. Ray, S.; Das, G. *Process Equipment and Plant Design: Principles and Practices*; Elsevier: Amsterdam, The Netherlands, 2020; p. 142.
16. Yeo, Y.S.; Alwi, S.R.W.; Ahmad, S.; Manan, Z.A.; Zamzuri, N.H. A New Graphical Method for Heat Exchanger Network Design Involving Phase Changes. *Chem. Eng. Trans.* **2017**, *56*, 1249–1254. [CrossRef]
17. Ponce-Ortega, J.M.; Serna-González, M.; Jiménez-Gutiérrez, A. Synthesis of Heat Exchanger Networks with Optimal Placement of Multiple Utilities. *Ind. Eng. Chem. Res.* **2010**, *49*, 2849–2856. [CrossRef]
18. Na, J.; Jung, J.; Park, C.; Han, C. Simultaneous Synthesis of a Heat Exchanger Network with Multiple Utilities Using Utility Substages. *Comput. Chem. Eng.* **2015**, *79*, 70–79. [CrossRef]
19. Papoulias, S.A.; Grossmann, I.E. A Structural Optimization Approach in Process Synthesis—II. Heat Recovery Networks. *Comput. Chem. Eng.* **1983**, *7*, 707–721. [CrossRef]
20. Shenoy, U.V.; Sinha, A.; Bandyopadhyay, S. Multiple Utilities Targeting for Heat Exchanger Networks. *Chem. Eng. Res. Des.* **1998**, *76*, 259–272. [CrossRef]
21. Briones, L.; Escola, J.M. Application of the Microsoft Excel Solver Tool in the Solution of Optimization Problems of Heat Exchanger Network Systems. *Educ. Chem. Eng.* **2019**, *26*, 41–47. [CrossRef]
22. Towler, G.; Sinnott, R. *Chemical Engineering Design: Principles, Practice and Economics of Plant and Process Design*; Butterworth-Heinemann: Oxford, UK, 2008; p. 140.
23. Di Pretoro, A.; Manenti, F. *Non-Conventional Unit Operations: Solving Practical Issues*; Springer: Cham, Switzerland, 2020; p. 6.
24. Kemp, I.C.; Lim, J.S. *Pinch Analysis for Energy and Carbon Footprint Reduction: User Guide to Process Integration for the Efficient Use of Energy*, 3rd ed.; Butterworth-Heinemann: Oxford, UK, 2020; pp. 529–530.
25. Walmsley, T.G.; Lal, N.S.; Varbanov, P.S.; Klemeš, J.J. Automated Retrofit Targeting of Heat Exchanger Networks. *Front. Chem. Sci. Eng.* **2018**, *12*, 630–642. [CrossRef]
26. Sinnott, R.K. *Coulson & Richardson's Chemical Engineering*, 3rd ed.; Butterworth-Heinemann: Burlington, VT, USA, 1999; p. 107.
27. Chang, C.; Chen, X.; Wang, Y.; Feng, X. Simultaneous Synthesis of Multi-Plant Heat Exchanger Networks Using Process Streams across Plants. *Comput. Chem. Eng.* **2017**, *101*, 95–109. [CrossRef]
28. McFedries, P. *Microsoft Excel 2019: Formulas and Functions*; Pearson Education: New York, NY, USA, 2019; p. 429.
29. Hollis, P.C. *Energy from Waste & Biomass Fuels*; AuthorHouse: Bloomington, IN, USA, 2014; p. 102.
30. Mizutani, F.T.; Pessoa, F.L.P.; Queiroz, E.M.; Hauan, S.; Grossmann, I.E. Mathematical Programming Model for Heat-Exchanger Network Synthesis Including Detailed Heat-Exchanger Designs. 2. Network Synthesis. *Ind. Eng. Chem. Res.* **2003**, *42*, 4019–4027. [CrossRef]
31. Liu, L.L.; Du, J.; Xiao, F.; Chen, L.; Yao, P.J. Direct Heat Exchanger Network Synthesis for Batch Process with Cost Targets. *Appl. Therm. Eng.* **2011**, *31*, 2665–2675. [CrossRef]
32. Serth, R.W.; Lestina, T. *Process Heat Transfer*, 2nd ed.; Elsevier: Oxford, UK, 2014; p. 159.
33. Feng, Y.; Rangaiah, G.P. Evaluating Capital Cost Estimation Programs. *Chem. Eng.* **2011**, *118*, 22–29.
34. Chemical Engineering. Available online: https://www.chemengonline.com/plant-cost-index-beta/ (accessed on 19 May 2023).
35. Stijepovic, M.Z.; Linke, P. Optimal Waste Heat Recovery and Reuse in Industrial Zones. *Energy* **2011**, *36*, 4019–4031. [CrossRef]
36. Chen, Y.H.; Li, Y.W.; Chang, H. Optimal Design and Control of Solar Driven Air Gap Membrane Distillation Desalination Systems. *Appl. Energy* **2012**, *100*, 193–204. [CrossRef]
37. Sieniutycz, S.; Jezowski, J. *Energy Optimization in Process Systems and Fuel Cells*, 2nd ed.; Elsevier: Amsterdam, The Netherlands, 2013; p. 602.
38. Das, D.K.; Prabhudesai, R.K. *EIT Chemical Review*, 2nd ed.; Dearborn Real Estate Education: Austin, TX, USA, 2004.
39. Coker, A.K.; Sotudeh-Gharebagh, R. *Chemical Process Engineering*; Wiley: Hoboken, NJ, USA, 2022; p. 991.
40. Smith, R. *Chemical Process Design and Integration*, 2nd ed.; Wiley: Chichester, UK, 2016; p. 503.
41. Seider, W.D.; Lewin, D.R.; Seader, J.D.; Widagdo, S.; Gani, R.; NG, K.M. *Product and Process Design Principles*, 4th ed.; Wiley: Hoboken, NJ, USA, 2017; p. 333.

42. Çengel, Y.A.; Boles, M.A.; Kanoğlu, M. *Thermodynamics: An Engineering Approach*, 10th ed.; McGraw-Hill: New York, NY, USA, 2023; pp. 307–308.
43. Jiang, N.; Shelley, J.D.; Doyle, S.; Smith, R. Heat exchanger network retrofit with a fixed network structure. *Appl. Energy* **2014**, *127*, 25–33. [CrossRef]